SPATIAL AND RADIOMETRIC QUALITY OF THE MOSAIC OF IMAGES ACQUIRED BY AIRBORNE DIGITAL VNIR MATRIX CAMERA AND TIR LINE SCANNER

A. Krtalić*, T. Fiedler**

*University of Zagreb, Faculty of Geodesy, 10000 Zagreb, andrija.krtalic@zg.htnet.hr
**University of Zagreb, Faculty of Geodesy, 10000 Zagreb, teodor.fiedler@zg.htnet.hr

KEY WORDS: mosaic, geocoding, digital parallel scan camera, digital matrix camera, geometric deviation, radiometry deviation

ABSTRACT:

The analogue aerial photo cameras are using the panchromatic, color visible, color infrared film and dominate in wide area photogrammetric data acquisition but also digital cameras became available on the market. Digital airborne sensors offer new technical and opperational opportunities although require new approaches, knowledge, education and training. While very suitable and efficient in use the digital airborne sensors bring new problems that should be solved for best quality of their products. In this paper we consider the quality of spatial and radiometric features of the mosaic of images acquired by two digital airborne sensors that have different modes of image formation and work at different wavelenghts. The first sensor is the digital matrix (staring) camera, for three visible channels (V: 0.4–0.5 µm, 0.5-0.6 µm, 0.6-0.7 µm), for near infrared channel (NIR: 0.7-1.0 µm) and the second sensor is the longwave thermal infrared (TIR: 8-14 µm) parallel scan camera. Although for TIR wavelengths exist matrix cameras they have rather limited resolution (320x240 pixels) and the parallel scan cameras are in intensive use due to better resolution. The both sensors are in intensive operational use in Croatia, and this was the motif for this analysis. We analyse spatial and radiometric quality of the mosaic of high resolution VNIR images (1392x1040 pixels) and of TIR images (600x400 pixels). If compared to VNIR images, TIR images have spatial distorsions due to parallel scanning mode. For the case study was selected the scene that has small number of objects that could be used for registration of TIR images onto VNIR images. The work is part of the research conducted in the scientific project ARC funded by European Commission.

1 INTRODUCTION

Operative system which consist of two sensors, two digital cameras, DuncanTech MS3100 and Thermovision THV 1000, are in intesive operational use in Croatia for remote sensing of minefields. The first sensor is the digital matrix camera, for acquisition in three visible channels (V: 0.4-0.5 µm, 0.5-0,6 µm, 0.6-0.7 µm) and near infrared (NIR: 0.7-1.0 µm) and the second sensor is parallel scan camera which collects data in the longwave thermal infrared (TIR: 8-14 µm) area. These two cameras are different in many ways, they collect data in different wavelengths and they have different principle of collecting data. DuncanTech MS3100 is the digital matrix camera (sensor resolution 1392x1040 pixels) and it produces images in central projection. Thermovision THV 1000 collects the data by scaning 5 parallel lines at the time in 80 rows with resolution of sensor 5x400 pixels. The reason for this particular camera to be used instead of matrix camera (available in the market) is the sensor resolution. The matix TIR cameras have resolution of 320x240 pixels and for that reason parallel scan camera is in use. The flights for collecting the images for the purpose of humanitarian demining in Croatia took place at the height of 130 m and higher above the ground. Because of small flight height, the small surface of each image and a large number of images, the orientation in space has become more difficult. This problem can be solved by mosaicing the selected images of the an area and geocoding of the whole mosaic. However, these proceses generate new problems, as additional geometric and radiometric deformation of images made by interpolation in mosaicing and geocoding. Therefore, for the practicle use of mosaic, it is necessary to know what can we expect from it with respect to geometric improvement and radiometric distortions. This is important especially for TIR mosaic because of considerable geometric deformations of original (input) images. For that purpose the comparison of geometric and radiometric relationships between original images and geocoding mosaics was done.

2 GEOMETRIC COMPARISON OF IMAGES

2.1 Selection of a pair of images and equalizing of scale

For geometric comparison there was a pair of images selected (one VNIR and one TIR) with the biggest owerlap between images and the biggest quantity of details which can be detected on both images. The end points of both images were defined by their sensor resolutins and images were interactivly positioned between those points. Thus, a common unit of measurement (for both images) is a pixel. On both images there were 8 identical details identified so that certain details on VNIR image can be joined with two parallel horizontal and two parallel vertical lines (lines that are parallel with the axes of coordinate system).

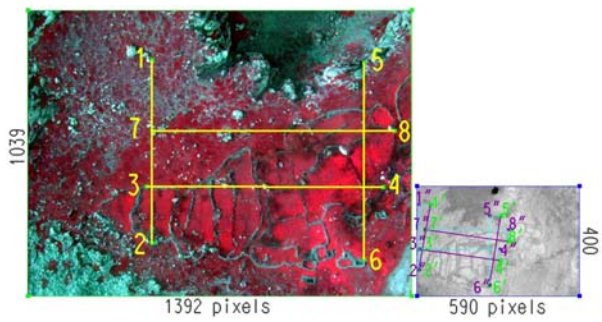

Figure 1. Delineated identical points on the pair of images, VNIR (left) and TIR (right), with 60% overlap

The lines between the same points on TIR image aren't horizontal and vertical because of parallel scaning and moving of platform (helicopter), they are inclined. Diferent resolutions of sensors for comparison those two images and true value of deformations between them call for equalizing of the scale (the most approximate scale). It is achieved by projecting the inclined lines of TIR image on to horizontal and vertical lines (parallel with coordinate axes) on VNIR image. After that, the projections on TIR image and the lines on VNIR image were measured and the coefficient for multiplication with rows K_y and columns K_x on TIR image was determined. Both images have approximately the same scale.

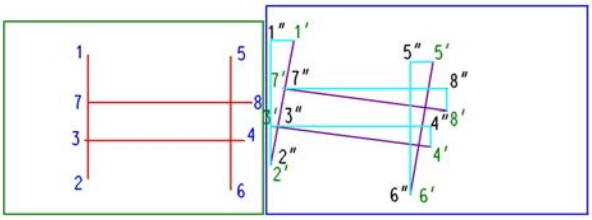

Figure 2. VNIR and TIR images at approximately the same scale

The coefficient was determined by means of the arithmetic mean between two relationships of horizontal and vertical lines.

1-2 = 663.85 pixels	1"-2" = 238.05 pixels
3-4 = 858.15 pixels	3"-4" = 292.05 pixels
5-6 = 715.76 pixels	5"-6" = 253.43 pixels
7-8 = 879.02 pixels	7"-8" = 301.45 pixels

K_y = 2.807 pxsels K_x = 2.926 pixels

2.2. Overlaping of identical part of images

After changing the scale of TIR image, differences between horizontal lines were (on Y axis) 3.20 and –3.03 pixels, (on X axis) –4.24 and 4.51 pixels. This value must be taken into further consideration of the size of deformations. As the reference point for TIR and VNIR images was selected the lowest possible detail which can be detected in lower left corner of TIR image (point 2), because of the assumption that deformations start at the beginning of the parallel scan image formation. Now, when the images are overlapping at approximately the same scale, they can be compared.

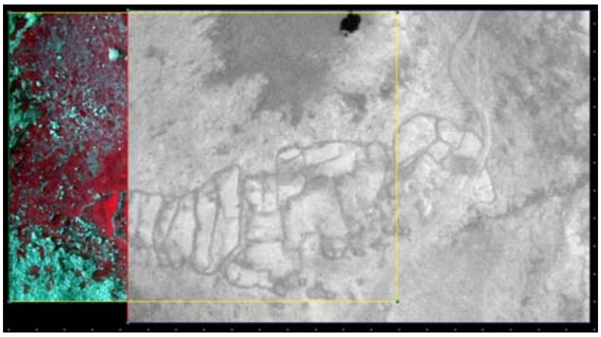

Figure 3. Overlap of images (yellow line shows the area of overlapping).

2.3. Vectorization of identical line elements on both images

For the purpose of comparing the position of the same details on both images, the vectorisation of line elements on the overlap area was done on both images. That vectorisation shows geometrical deviation between images (VNIR image in central projection and TIR image in parallel scaning mode).

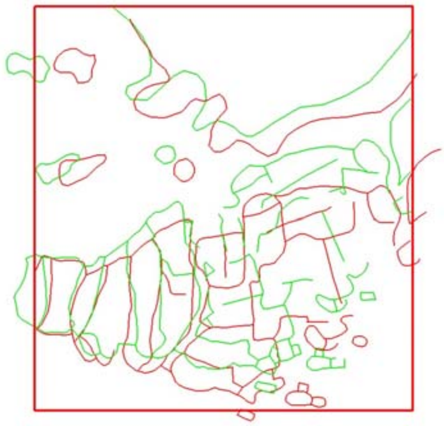

Figure 4. Distinction between maping contents on VNIR (green) and TIR (red) image after overlapping.

In order to present vector deviation of each detail on TIR image as related to an identical detail on VNIR image, the five vertical and five horizotal lines on VNIR images were selected and their positions on TIR image were found.

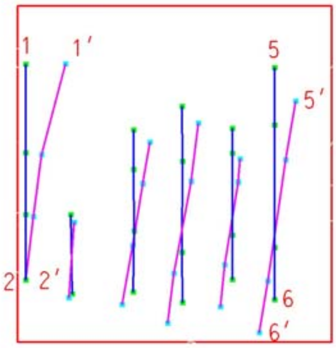

Figure 5. The blue lines are vertical lines on VNIR image and the purple lines show position of these lines on TIR image.

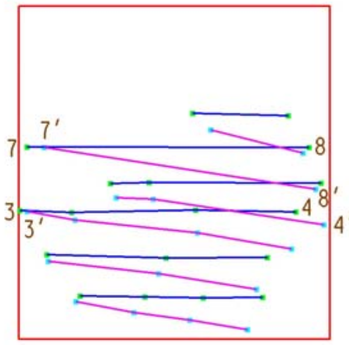

Figure 6. The blue lines are horizontal lines on VNIR image and the purple lines show position of these lines on TIR image.

The position deviation of details on TIR image as related to VNIR image was presented with deviation vector.

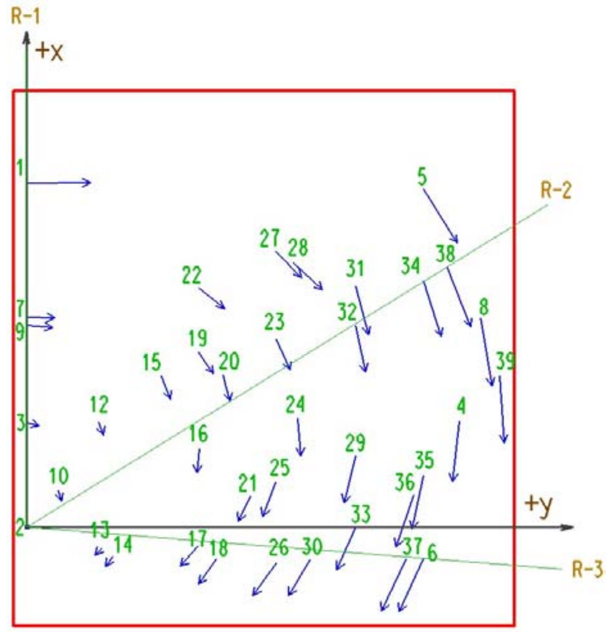

Figure 7. Deviation vectors of details on TIR image regarding the same details on VNIR image.

Let's put the pencil of rays in referenc point (point 2) and note that deformation of details on TIR image are getting bigger with larger distance of details from the origin of pencil. This regularity relates to particular ray only, because vectors of position deviation aren't parpendicular to the rays of pencil but the angle between a ray and a vector has become significantly larger with bigger distance from the point of origin of pencil on particular ray. For example, point 5 has the largest distance from the point of origin of pencil, 1010.4 pixels, but the deformation in this point (122.8 pixels) is not the biggest, the biggest deformation (132.5 pixels) is in the point 8 which is 968.2 pixels far away from the point of origin. Thus, the angle between particular vector of deviation of details on TIR image and the ray pencil pasing though the identical detail on VNIR image is increasing from the point of origin along the ray, as well as the size of vector of position deviation. In order to illustrate the above mentioned let's see some distances from the point of origin of pencil, the angles between vectors of position deviation and the ray and values of vector of position deviation of some points.

RAY	POINT	DISTANCE	ANGLE	DEVIATION
R-1	3	203.1 pixels	75°2371	24.1 pixels
	7	406.8 pixels	89°2197	54.3 pixels
	1	666.3 pixels	90°8247	123.7 pixels
R-2	32	747.6 pixels	69°9053	90.0 pixels
	34	904.6 pixels	75°9758	113.6 pixels
	38	956.9 pixels	80°1320	125.1 pixels
R-3	17	333.1 pixels	53°7550	50.9 pixels
	30	552.3 pixels	63°5036	80.5 pixels
	6	770.6 pixels	69°4388	113.8 pixels

The increase of vectors of deviation on vertical axis (X) is the biggest per unit of length (have fastest increase), and the increase of coordinate Y causes the rotation of vector of deviation toward the point of origin of tuft, so that the deformation of TIR image in relation to VNIR image have tendency of irregulator circular moving around the point of origin of tuft of rays. Points on the vertical lines at VNIR image appear at TIR image on both sides of the projection of VNIR vertical lines in the area of overlapping these two images and the fictitious connector of these points intersects with the VNIR vertical line. Vector of deviation in intersection point has got the direction along fictitious connector of deformation points at TIR image.

3. MOSAICKING AND GEOCODING OF MOSAICS

For mosaicking there were 5 VNIR and 5 TIR images chosen which were snapshots in two strips in same period of time. VNIR and TIR images covered approximately the same surface of the terrain. The first step was mosaicking along the strip and after that mosaiking between strips was done. After mosaicking, the both mosaics were geocoded by means of the software package DESCARTES with Thin Plate Spline transformation according to digital orthophoto (DOF) of the same area. The size of pixel on DOF is 0.5 m. Geocoding the VNIR mosaic was done on 232 common points, TIR mosaik on 96 common points. The main problem with mosaicking and geocoding, was in finding the sufficient number of good details on TIR images in order to perform the above mentioned operations as well as possible,and to analyse the deviation from DOF image.

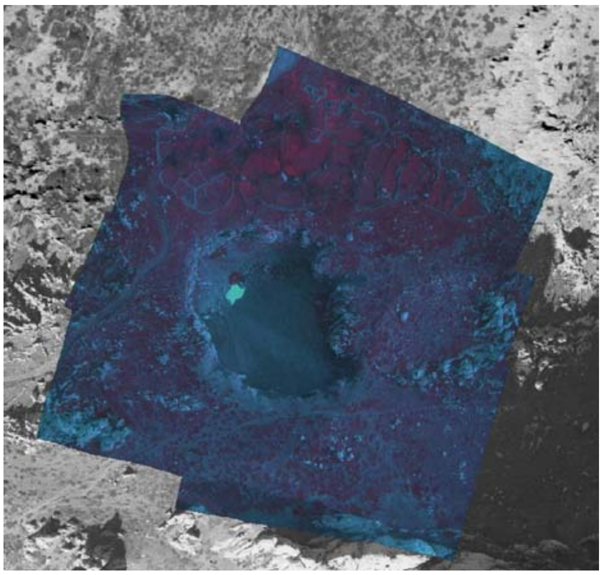

Figure 8. Geocoding VNIR mosaic over DOF image.

Figure 9. Geocoding TIR mosaic over DOF image.

The quality of geocoding was checked on 52 points on all three images and the mean deviations of points on both axes, related to DOF are:

TIR

$$M''_y = \pm 0.9 \text{ m} \quad M''_x = \pm 1.1 \text{ m} \qquad (1)$$

VNIR

$$M'_y = \pm 0.6 \text{ m} \quad M'_x = \pm 0.4 \text{ m} \qquad (2)$$

The mean deviations of position are:

$$M''_p = \pm 1.5 \text{ m} \qquad (3) \qquad\qquad M'_p = \pm 0.7 \text{ m} \qquad (4)$$

When the TIR mosaic was compared with VNIR mosaic, it resulted in the following values:

$$M_y = \pm 1.0 \text{ m} \quad M_x = \pm 1.1 \text{ m} \quad M_p = \pm 1.5 \text{ m} \qquad (5)$$

The selection of checking points for the quality of geocoding stipulates TIR image because the good identical details are more difficult to recognise on TIR then on VNIR and DOF.

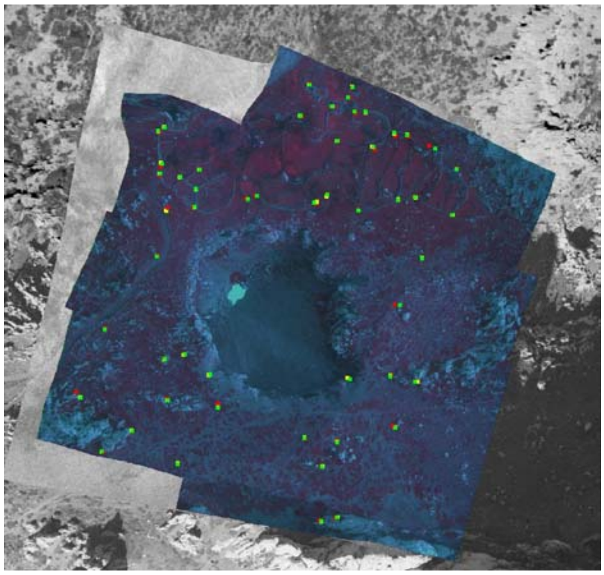

Figure 10. Overlapping of DOF, VNIR and TIR images with marked identical points for the analysis of deviation.

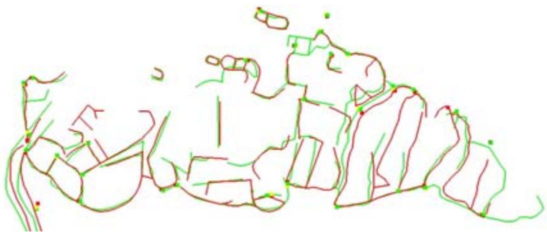

Figure 11. Comparison of maping contents VNIR (green) and TIR (red) details after geocoding.

4. RADIOMETRY

Geocoding has improved the quality of geometrical relationships between the details on mosaics, but it has to be determined what happened with radiometry regarding to interpolation during the mosaicking and geocoding. VNIR images in mosaic are RGB images (blue, green and infra red channel). For analysing radiometric quality of mosaics the comperison of histograms of 3 samples from geocoding mosaics with histograms of original images which show the same area like the samples do, was done.

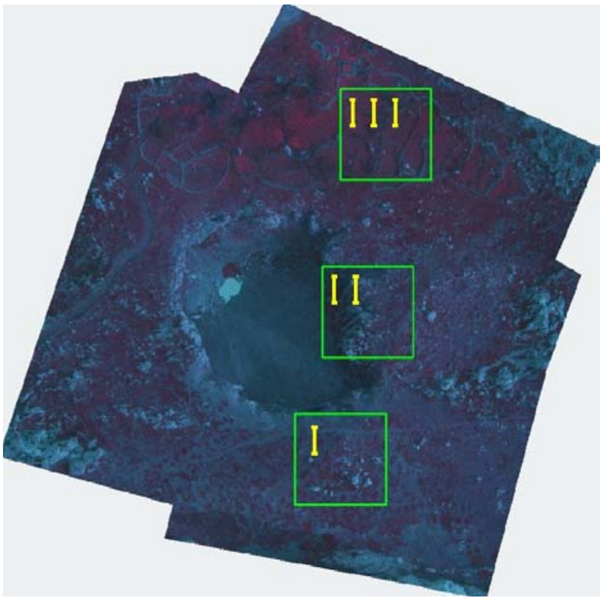

Figure 12. Geocoding VNIR mosaic with marked samples.

The samples show approximately the same area on every image from which they have been taken for monitoring radiometric and geometric deformation during mosaicking and improvement of geometrical relationships during geocoding. The samples I and III have been token into consideration because I sample was unchanged and sample III had the biggest deformation in geometric and radiometric domain because that sample is the furthest from the first image in mosaic.

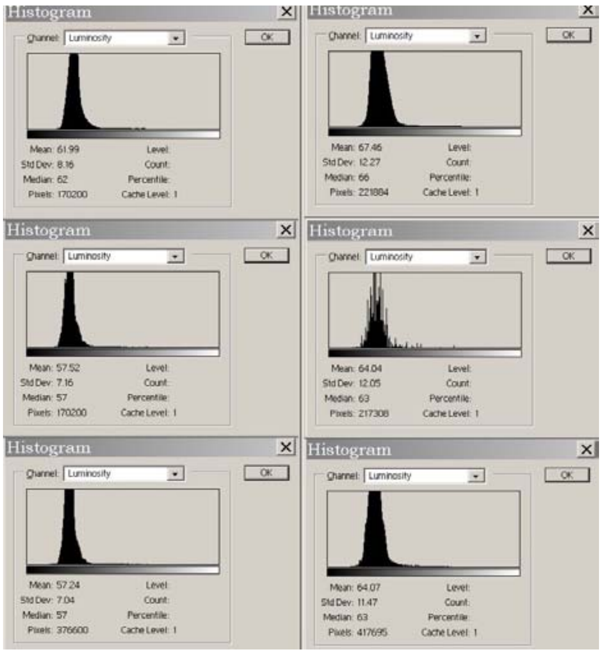

Figure 13. Comparison between histogram of part of original VNIR RGB image (up left – I sample, up right – III sample), histogram of the same area, not geocoding RGB mosaic (in the middle left – I sample, in the middle right – III sample) and histogram of geocoding RGB mosaic (down left – I sample, down right – III sample).

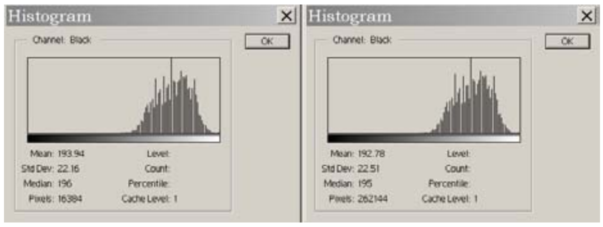

Figure 14. Comparison between histogram of part of original TIR image (left) with histogram of geocoding TIR mosaic (right), sample corresponds to III sample from VNIR mosaic.

SAMPLE	NUM. OF PIXELS	MEAN	ST.DEV.	MEDIAN
VNIR				
I – image	460x370	61.99	8.16	62
I – mosaic	460x370	57.52	7.16	57
I – geo_mos	700x538	57.24	7.04	57
III–image	442x502	67.46	12.27	66
III–mosaic	398x546	64.04	12.05	63
III–geo_mos	601x695	64.07	11.47	63
TIR				
III–image	128x128	193.94	22.16	196
III–geo_mos	512x512	192.78	22.51	195

This data show that the information on TIR image change a little as related to original image, in spite of fact that number of pixel have significantly increased by geocoding, and the differences on VNIR images are more significant and their influence can be visible on shape of histogram and MEAN and MEDIAN values between original image and geocoding mosaic.

5. CONCLUSION

Mosaics which were produced from digital images of DuncanTech MS3100 and Thermovision THV 1000 are useful information for the orientation on snapshot area and give possibility for radiometric analysis of data on entire snapshot area at the same time. Geometric deformation of details can be improved by geocoding. The mean value of deviation of details on VNIR and TIR geocoded mosaics related to DOF show that fact, that it is possible to make joint radiometric analysis (i.e. the classification which can be done because the pixel size is the same on both mosaics) with biggest tolerance of results. The deviation of VNIR geocoding mosaik regarding the model (DOF 1:5000) are fully satisfying geometrical accuracy of DOF 1:5000 ((2) and (4)), because there aren't any deviation larger than 1.5 m on both axes. Standard deviations of TIR mosaic, regarding the model (DOF 1:5000), are also within the accuracy of DOF 1:5000 ((1) and (3)), but 4 points have y coordinate and 6 points have x coordinate deviation bigger than 1.5 m. In this case one should take into consideration the fact that the radiometric data VNIR of geocoded mosaic differ much from their original copies that they have been made of, than it was the case with TIR geocoded presentation. Base for geocoding was DOF 1:5000 with pixel size of 0.5 m. If we had better base for geocoding (smoller pixels of base image), geometric transformation would give better results. For the radiometric analysis it is necessary to find the adequate methods of comparison.

6. REFERENCES

Krauss, K., 1997. *Photogrammety Volume I, II.* Dűmler, Bonn

Moffit, F. H., Mikhail, M. E., 1980. *Photogrammetry.* Harper & Row, Publishers, New York

Castlelman, R. K., 1997. *Digital Image Procesing.* Prentice-Hall International, Inc.

Kasser, M., Yves E., 2002. *Digital photogrammetry.* Taylor & Francis, London

Olujić, M., 2001. *Snimanje i istraživanje Zemlje iz svemira, sateliti,senzori, primjena.* HAZU i GEOSAT, Zagreb

Fail, L., 1989. *Teorija pogrešaka i račun izjednačenja.* Geodetski fakultet, Zagreb

DuncanTech, *MS3100 Digital Multispektral Camera.* Auburn